THE HIPPARCOS HERTZSPRUNG-RUSSELL DIAGRAM OF S STARS: PROBING NUCLEOSYNTHESIS AND DREDGE-UP

S. Van Eck[1], A. Jorissen[1], S. Udry[2], M. Mayor[2], B. Pernier[2]

[1]Institut d'Astronomie et d'Astrophysique, U.L.B., C.P.226, Boulevard du Triomphe, B-1050 Bruxelles, Belgium
[2]Observatoire de Genève, 51 Chemin des Maillettes, CH-1290 Sauverny, Switzerland

ABSTRACT

Hipparcos parallaxes are used to construct the HR diagram of a sample of 30 S stars with $\sigma_\pi/\pi < 0.85$. *Extrinsic* (i.e. Tc-poor, binary) S stars are bluer and fainter than *intrinsic* (i.e. Tc-rich) S stars. The comparison with theoretical evolutionary tracks indicates that Tc-rich S stars appear at the onset of thermal pulses on the asymptotic giant branch. A comparison is also made with the Magellanic Cloud S and C stars.

Key words: S stars; AGB stars; Hertzsprung-Russell diagram; stellar evolution; fundamental parameters.

1. THE INTRINSIC-EXTRINSIC PARADIGM

S stars are late-type giants exhibiting ZrO bands on top of the usual TiO bands found in normal M giants. Elements heavier than Fe are overabundant, with the distinctive signature of the s-process nucleosynthesis (Smith & Lambert 1990). Previous studies (e.g. Little et al. 1987; Brown et al. 1990; Jorissen & Mayor 1992) have identified *two kinds of S stars*, depending on the presence or absence of lines of technetium (Tc), an element with no stable isotopes: Tc-rich S stars supposedly owe their chemical peculiarities to *internal nucleosynthesis* associated with thermal pulses on the asymptotic giant branch (AGB), whereas Tc-poor S stars presumably owe their chemical peculiarities to *mass transfer* in a binary system. Tc-poor S stars are believed to be the cooler analogs of barium stars. More precisely, the (main-sequence) progenitor of the current chemically-peculiar giant (i.e. Ba or Tc-poor S) accreted s-processed matter from its former AGB companion (now a white dwarf).

2. THE DATA SAMPLE

The Hipparcos catalogue comprises 62 stars from the *General Catalogue of Galactic S Stars* (Stephenson 1984): 20 Tc-rich, 21 Tc-poor, and 21 with unknown Tc (among which one star misclassified as S).

3. THE HERTZSPRUNG-RUSSELL DIAGRAM

3.1. Colours and Bolometric Magnitudes

In order to derive the absolute bolometric magnitudes, magnitudes from the UV to the far IR domain have been collected from the literature, de-reddened (Koornneef 1983), and converted to monochromatic fluxes using the zero-magnitude fluxes of Johnson (1966). The bolometric correction is then either calculated by integrating, when all are available, the $UBVRIJHKLM$ fluxes, the infrared fluxes from the Revised Air Force Four-Colour Infrared Sky Survey (Price & Murdock 1983) and the IRAS fluxes, or derived from the $(BC_{\rm K}, (V-K)_0)$ relation of Bessell & Wood (1984) applicable to oxygen-rich stars. For the 17 S stars where both methods are applicable, they yield consistent results (with a rms deviation of 0.1 mag). The $(V-K)_0$ colour index is used as a temperature indicator (Ridgway et al. 1980). More details can be found in the full paper (Van Eck et al. 1997a).

3.2. The HR Diagram of S Stars

Figure 1 presents the HR diagram of the 30 stars with useful parallaxes ($0 < \sigma_\pi/\pi < 0.85$) and adequate photometry available. A segregation between extrinsic and intrinsic S stars is readily apparent, with extrinsic S stars being intrinsically fainter and bluer than intrinsic S stars.

Part of the overlap in luminosity between extrinsic and intrinsic S stars may actually be attributed to the large error bars of the interloping stars, as can be seen on Figure 2, presenting (separately for intrinsic and extrinsic S stars) the range of $M_{\rm bol}$ corresponding to $\pi \pm \sigma_\pi$.

4. COMPARISON WITH THEORETICAL EVOLUTIONARY TRACKS

Figures 3 and 4 compare the position of S stars in the HR diagram with theoretical evolutionary tracks of

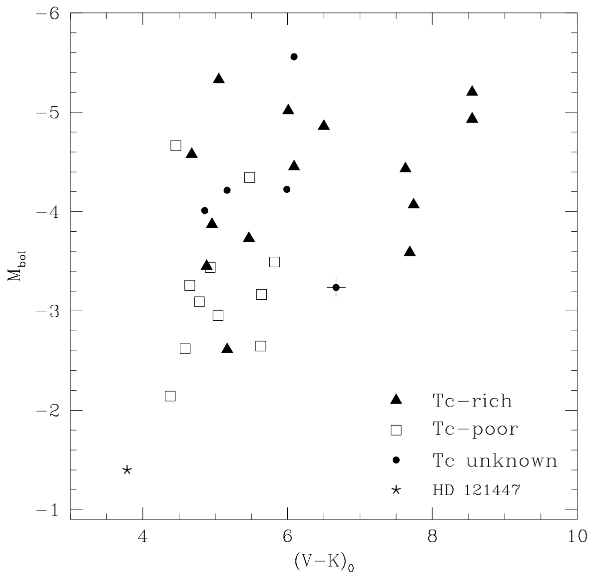

Figure 1. The HR diagram for S stars with useful parallaxes ($0 < \sigma_\pi/\pi < 0.85$). HD 121447, the boundary case between Ba and S stars (see Section 4), is represented by $\star$. The close visual binary HIP 19853 is represented by +.

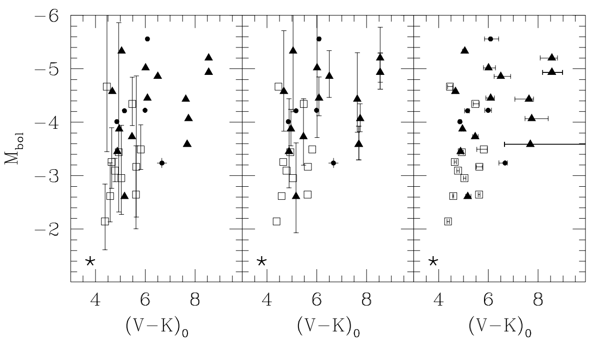

Figure 2. The uncertainty on M_{bol} due to the uncertainty σ_π on the parallax π. The error bar extends from $M_{bol}(\pi+\sigma_\pi)$ to $M_{bol}(\pi-\sigma_\pi)$. Left panel: Tc-poor S stars; middle panel: Tc-rich S stars. Right panel: the uncertainty on V–K caused by the intrinsic variability of S stars in the Hipparcos Hp magnitude; the error bar covers the range in Hp between the 5th and 95th percentiles. Symbols are as in Figure 1.

the first giant branch (RGB) and of the early asymptotic giant branch (E-AGB; prior to the first thermal pulse), respectively.

The predicted location of the giant branch in the HR diagram is known to depend sensitively upon model parameters like the convective mixing length or the atmospheric opacities. For the Geneva evolutionary tracks used here, these model parameters have been calibrated so as to reproduce the observed location of the red giant branches of more than 75 clusters (Schaller et al. 1992). The comparison of these tracks

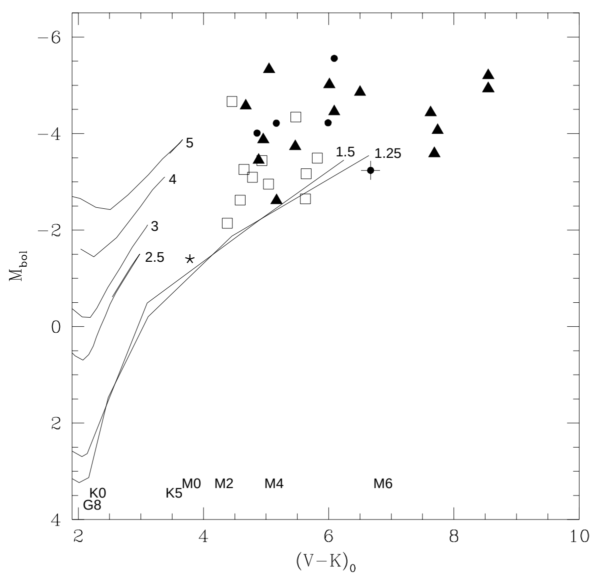

Figure 3. The location of the RGB for stars of various masses (as labelled, in $M_\odot$) and metallicity $Y = 0.3$, $Z = 0.02$, up to the onset of core He-burning, according to Schaller et al. (1992). Equivalent spectral types are given on the bottom scale.

with the observed location of S stars in the HR diagram is thus meaningful.

The main result of the present study is apparent on Figure 4: the line marking the onset of thermal pulses matches well the limit between intrinsic and extrinsic S stars, so that *Tc-rich intrinsic S stars may be associated with thermally-pulsing AGB stars.*

The previous result provides interesting constraints on the occurrence of both the s-process and the third dredge-up in thermally-pulsing AGB stars, by suggesting that those processes operate from the very first thermal pulses on, a conclusion already reached by several authors (e.g. Richer 1981) from the luminosity function of carbon stars in the Magellanic Clouds (see, however, the discussion of Section 5). Because there is little change in luminosity from one pulse to the next (see Figure 4), and because of the uncertainties affecting the location of individual S stars in the HR diagram, it is difficult, however, to set a precise limit on the exact number of pulses necessary to change a normal M giant into an (intrinsic) S star.

As far as extrinsic S stars are concerned, the present data alone do not permit to distinguish between them populating the RGB or the E-AGB of low-mass stars. However, when both the RGB and the E-AGB are possible, evolutionary time-scale considerations clearly favor the RGB over the E-AGB. Orbital elements of extrinsic S stars (Jorissen et al. 1997) point towards them being low-mass stars, with an average mass of $1.7 \pm 0.2\ M_\odot$. This value is in excellent agreement with their position along the RGB of low-mass stars in Figure 3.

Contrary to what might be inferred from the smooth

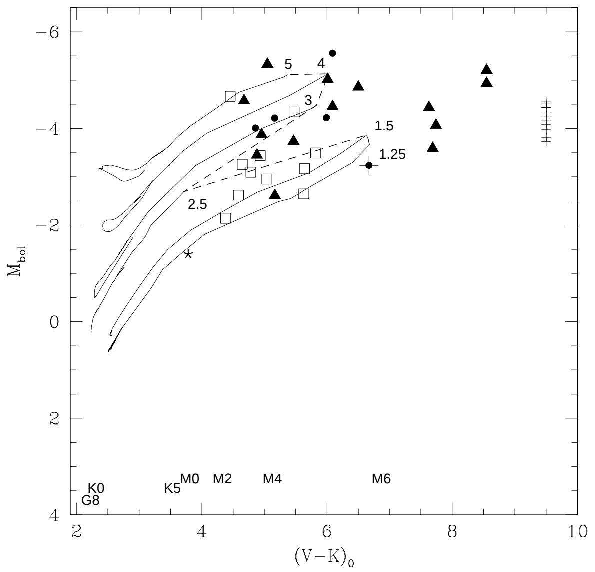

Figure 4. Same as Figure 3, but for the early-AGB up to the first thermal pulse (Charbonnel et al. 1996). The thermally-pulsing AGB thus extends rightwards from the dashed line. The crosses along the right-hand axis provide the luminosities of the first ten thermal pulses in a 1.5 $M_\odot$ star with LMC metallicity (i.e. Z = 0.008) computed by Wagenhuber & Tuchman (1996).

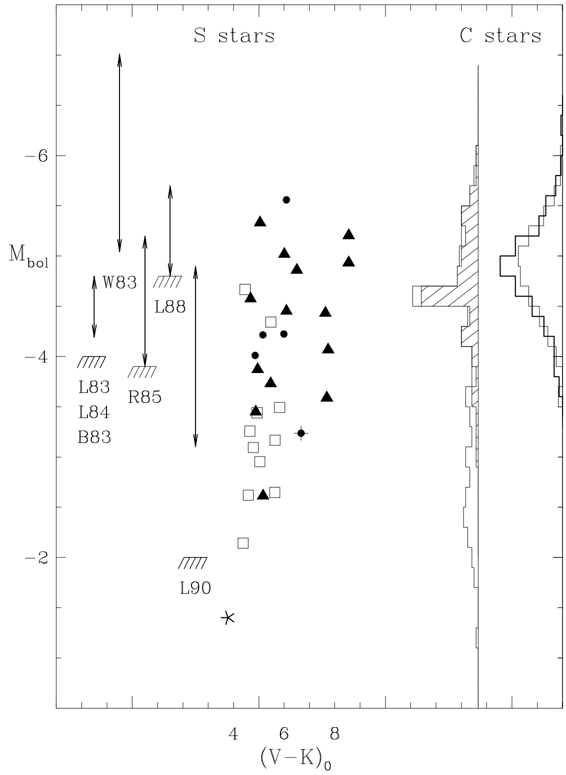

Figure 5. Comparison of the M_{bol} range of S stars in the solar neighborhood (this work, symbols are as in Figure 1) and in external systems. For the S stars: Magellanic Cloud clusters: L83 (Lloyd Evans 1983), L84 (Lloyd Evans 1984), B83 (Bessell et al. 1983); Magellanic Cloud field: W83 (Wood et al. 1983), R85 (Reid & Mould 1985), L88 (Lundgren 1988); Fornax dwarf elliptical galaxy: L90 (Lundgren 1990). Detection thresholds are also indicated. For the C stars: the rightmost histogram gives the luminosity function of the 186 LMC (thick line) and 134 SMC (thin line) C stars identified by Blanco et al. (1980). The leftmost histogram provides the luminosity functions of C stars from the Westerlund et al. (1991) SMC survey (hatched) as well as from the deeper Westerlund et al. (1995) SMC survey (open).

transition between intrinsic and extrinsic S stars in the HR diagram, the two kinds of S stars belong to distinct galactic populations. Their galactic latitude distributions are clearly distinct (Jorissen et al. 1993). This difference translates into scale heights above the galactic plane of about 180 and 600 pc for intrinsic and extrinsic S stars, respectively. This result (Van Eck et al. 1997b) was obtained for the Henize sample of 205 S stars by adopting $\langle M_v \rangle = -2$ and -1 for intrinsic and extrinsic S stars, respectively, in fair agreement with the present results. Extrinsic and intrinsic S stars are thus not simply successive stages along the evolution of stars in the same mass range.

Two extrinsic S stars, HD 35155 and 57 Peg, are brighter than $M_{bol} = -3.5$ and deserve further comments. HD 35155 is the extrinsic S star with the second largest relative error on the parallax (see Figure 2). This binary extrinsic S star has an orbital period of 642 ± 3 d (Jorissen & Mayor 1992) in a nearly circular orbit, yielding an orbital separation of about 2 AU assuming typical masses of 1.7 $M_\odot$ for the S star and 0.6 $M_\odot$ for its suspected white dwarf companion (see Jorissen et al. 1997). The corresponding angular separation on the sky (a) will thus be about twice the annual parallax (since $a = A\pi$, when A is the orbital separation expressed in AU). Since the orbital period is moreover of the order of the duration of the Hipparcos mission, this system poses a difficult challenge to the reduction process.

57 Peg is a long-period binary system with a composite IUE spectrum caused by an A6V companion of mass 1.9 $M_\odot$ (assuming $M_v = +2.05$ for A6V stars, and given the Hipparcos parallax). The S star primary must have evolved faster and should thus be more massive than 1.9 $M_\odot$, which is consistent with its position in the HR diagram along the 3 $M_\odot$ E-AGB track (Figure 4). That S star is thus likely to be more massive than the average extrinsic S star (for which $\langle M \rangle = 1.7 \pm 0.2$ $M_\odot$; Jorissen et al. 1997). Although this solution is consistent with the position of 57 Peg in the HR diagram, it is incompatible with the binary paradigm, which requires white dwarf (WD) companions for Tc-poor stars. The only possibilities to resolve this puzzle within the framework of the binary paradigm for extrinsic S stars is either that 57 Peg is a triple system (S+A6V+WD) or that it is not an S star at all.

Finally, note that the lower left boundary of the region occupied by extrinsic S stars is set by the condition that T_{eff} be low enough in order that ZrO bands may form. Such a threshold roughly corresponds to the transition between K and M giants (see the spectral-type labels in Figure 3), so that extrinsic S stars should merge into the KIII barium stars at lower luminosities and bluer colours along the RGB (e.g. Jorissen et al. 1997). As an example, the transition object HD 121447, classified either as K7IIIBa5 (Lü 1991) or S0 (Keenan 1950), has been located in Figure 3 following the methods presented in Section 3.1 and using its Hipparcos parallax as provided by Mennessier et al. (1997).

5. COMPARISON WITH S AND CARBON STARS IN EXTERNAL SYSTEMS

Several S stars have been found in the Magellanic Clouds and in a few other nearby galaxies, allowing a direct comparison of their luminosities with those derived from the Hipparcos trigonometric parallaxes for galactic S stars (Figure 5). S stars in the external systems have luminosities comparable to the galactic Tc-rich S stars. As far as Tc-poor S stars are concerned, their luminosity range is generally not covered by the existing surveys of S stars in the Clouds.

Deeper surveys are, however, available for carbon stars, because of their more conspicuous spectral features (Westerlund et al. 1995). The corresponding luminosity functions are also presented on Figure 5. The range of absolute bolometric magnitudes for carbon stars from the deeper SMC survey totally covers that of galactic S stars, including its low-luminosity tail. More precisely, the faint carbon stars uncovered by the deep Westerlund et al. (1995) SMC survey have luminosities similar to the extrinsic S stars in the solar neighborhood. The nature of the low-luminosity SMC carbon stars is still debated. They might be low-luminosity carbon stars equivalent to the galactic R carbon stars, or extrinsic carbon stars formed by mass transfer across a binary system like galactic extrinsic S stars (Barnbaum & Morris 1993).

6. CONCLUSIONS

Since Tc-rich and Tc-poor S stars were indistinguishable on the basis of low-dispersion spectrograms used for classification purposes, they were originally assigned to a single spectroscopic class defined by the presence of ZrO bands. These two groups of stars are, however, well separated in the HR diagram constructed from the Hipparcos parallaxes: Tc-poor S stars are fainter and bluer than Tc-rich S stars. This segregation confirms the earlier finding that the chemical peculiarities of these two kinds of S stars have different origins. From a comparison with theoretical evolutionary tracks, Tc-rich S stars may now unequivocally be associated with thermally-pulsing AGB (TP-AGB) stars, whereas Tc-poor S stars are located along the RGB (or E-AGB) of low-mass stars. The lowest luminosity at which Tc-rich S stars are observed is an important constraint for models predicting the occurrence of the s-process and the third dredge-up in TP-AGB stars.

ACKNOWLEDGMENTS

Support for this work is provided to S.V.E. by a F.R.I.A. (Belgium) grant. Partial financial support from the *Fonds National de la Recherche Scientifique* (Belgium, Switzerland) is gratefully acknowledged. A.J. is Research Associate, F.N.R.S. (Belgium).

REFERENCES

Barnbaum, C., Morris, M., 1993, Bull. American Astron. Soc., 182, (46)17

Bessell, M.S., Wood, P.R., Lloyd Evans, T., 1983, MNRAS, 202, 59

Bessell, M.S., Wood, P.R., 1984, PASP, 96, 247

Blanco, V.M., McCarthy, M.F., Blanco, B.M., 1980, ApJ, 242, 938

Brown, J.A., Smith, V.V., Lambert, D.L., et al., 1990, AJ, 99, 1930

Charbonnel, C., Meynet, G., Maeder, A., Schaerer, D., 1996, A&AS, 115, 339

Johnson, H.L., 1966, ARA&A, 4, 193

Jorissen, A., Mayor, M., 1992, A&A, 260, 115

Jorissen, A., Frayer, D.T., Johnson, H.R., Mayor, M., Smith, V.V., 1993, A&A, 271, 463

Jorissen, A., Van Eck, S., Mayor, M., Udry, S., 1997, A&A, submitted

Keenan, P.C., 1950, AJ, 55, 172

Koornneef, J., 1983, A&A, 128, 84

Little, S.J., Little-Marenin, I.R., Hagen-Bauer, W., 1987, AJ, 94, 981

Lloyd Evans, T., 1983, MNRAS, 204, 985

Lloyd Evans, T., 1984, MNRAS, 208, 447

Lü, P.K., 1991, AJ, 101, 2229

Lundgren, K., 1988, A&A, 200, 85

Lundgren, K., 1990, A&A, 233, 21

Mennessier, M.O., et al., 1997, A&A, in press

Price, S.D., Murdock, T.L., 1983. The Revised AFGL Infrared Sky Survey Catalog (AFGL-TR-83-0161)

Reid, N., Mould, J., 1985, ApJ, 299, 236

Richer, H.B., 1981, ApJ, 243, 744

Ridgway, S.T., Joyce, R.R., White, N.M., Wing, R.F., 1980, ApJ, 235, 126

Schaller, G., Schaerer, G., Meynet, G., Maeder, A., 1992, A&AS, 96, 269

Smith, V.V., Lambert, D.L., 1990, ApJS, 72, 387

Stephenson, C.B., 1984. The General Catalogue of Galactic S Stars, (Warner & Swasey Obs.), 3, 1

Van Eck, S., Jorissen, A., Udry, S., Mayor, M., Pernier, B., 1997a, A&A, in press

Van Eck, S., et al., 1997b. In: R. Wing (ed.) IAU Symp. 177, Kluwer, Dordrecht, in press

Wagenhuber, J., Tuchman, Y., 1996, A&A, 311, 509

Westerlund, B.E., Azzopardi, M., Breysacher, J., Rebeirot, E., 1991, A&AS, 91, 425

Westerlund, B.E., Azzopardi, M., Breysacher, J., Rebeirot, E., 1995, A&A, 303, 107

Wood, P.R., Bessell, M.S., Fox, M.W., 1983, ApJ, 272, 99